Mineralogical Magazine, February 2015, Vol. 79(1), pp. 171–189

As-bearing new mineral species from Valletta mine, Maira Valley, Piedmont, Italy: II. Braccoite, $NaMn_5^{2+}[Si_5AsO_{17}(OH)](OH)$, description and crystal structure

Fernando Cámara[1,2,*], Erica Bittarello[1,2], Marco E. Ciriotti[3], Fabrizio Nestola[4], Francesco Radica[5] and Marco Marchesini[6]

[1] Dipartimento di Scienze della Terra, Università degli Studi di Torino, via Tommaso Valperga Caluso 35, I-10125 Turin, Italy
[2] CrisDi, Interdepartmental Center for Crystallography, via Pietro Giuria 7, I-10125, Turin, Italy
[3] Associazione Micromineralogica Italiana, via San Pietro 55, I-10073 Devesi-Cirié, Turin, Italy
[4] Dipartimento di Geoscienze, Università degli Studi di Padova, via Giovanni Gradenigo 6, I-35131 Padova, Italy
[5] Dipartimento di Scienze Geologiche, Università degli Studi Roma Tre, largo San Leonardo Murialdo 1, I-00146 Rome, Italy
[6] EEEP house, UNIR, Basing View, Basingstoke, Hampshire RG21 4YY, UK

[*Received 15 May 2014; Accepted 27 July 2014; Associate Editor: S. J. Mills*]

ABSTRACT

The new mineral species braccoite, ideally $NaMn_5^{2+}[Si_5AsO_{17}(OH)](OH)$, has been discovered in the Valletta mine dumps, in Maira Valley, Cuneo province, Piedmont, Italy. Its origin is probably related to the reaction between ore minerals and hydrothermal fluids. It occurs as subhedral crystals in brown-red coloured thin masses, with a pale-yellow streak and vitreous to resinous lustre. Braccoite is associated with tiragalloite, for which new data are provided, as well as gamagarite, hematite, manganberzeliite, palenzonaite, quartz, saneroite, tokyoite, unidentified Mn oxides, organic compounds, and Mn arsenates and silicates under study.

Braccoite is biaxial positive with refractive indices $\alpha = 1.749(1)$, $\beta = 1.750(1)$, $\gamma = 1.760(1)$. It is triclinic, space group $P\bar{1}$, with $a = 9.7354(4)$, $b = 9.9572(3)$, $c = 9.0657(3)$ Å, $\alpha = 92.691(2)$, $\beta = 117.057(4)$, $\gamma = 105.323(3)^{\circ}$, $V = 740.37(4)$ Å^3 and $Z = 2$. Its calculated density is 3.56 g/cm^3. The ten strongest diffraction lines of the observed powder X-ray diffraction (XRD) pattern are [*d* in Å, (*I*), (*hkl*)]: 3.055 (69)($2\bar{2}1$), 3.042 (43)(102), 3.012 (65)($3\bar{2}\bar{1}$), 2.985 (55)($2\bar{3}\bar{1}$), 2.825 (100)($21\bar{3}$), 2.708 (92)(220), 2.627 (43)($2\bar{3}\bar{2}$), 2.381 (58)($4\bar{1}\bar{1}$), 2.226 (25)($21\bar{4}$) and 1.680 ($43\bar{3}$)(36). Chemical analyses by wavelength-dispersive spectroscopy electron microprobe gave (wt.%): Na_2O 4.06, CaO 0.05, MnO 41.76, MgO 0.96, Al_2O_3 0.04, CuO 0.02, SiO_2 39.73, As_2O_5 6.87, V_2O_5 1.43, SO_3 0.01 and F 0.04. H_2O 2.20 was calculated on the basis of 2OH groups p.f.u. Raman spectroscopy confirmed the presence of $(SiO_4)^{4-}$, $(AsO_4)^{3-}$ and OH groups. The empirical formula, calculated on the basis of Σ cations-(Na,K) = 11 p.f.u., in agreement with the results of the crystal structure, is $Na_{1.06}(Mn^{2+}_{4.46}Mn^{3+}_{0.32}Mg_{0.19}V^{3+}_{0.01}Al_{0.01}Ca_{0.01})[Si_5(As_{0.48}Si_{0.37}V^{5+}_{0.15})O_{17}(OH)](OH_{0.98}F_{0.02})$; the simplified formula is $Na(Mn,Mg,Al,Ca)_5[Si_5(As,V,Si)O_{17}(OH)](OH,F)$.

Single-crystal XRD allowed the structure to be solved by direct methods and revealed that braccoite is the As-dominant analogue of saneroite. The structure model was refined on the basis of 4389 observed reflections to $R_1 = 3.47\%$. Braccoite is named in honour of Dr Roberto Bracco (b. 1959), a systematic minerals collector with a special interest in manganese minerals. The new mineral was approved by the International Mineralogical Association Commission on New Minerals, Nomenclature and Classification (IMA 2013-093).

* E-mail: fernando.camaraartigas@unito.it
DOI: 10.1180/minmag.2015.079.1.14

Keywords: braccoite, saneroite, arseno-silicates, tiragalloite, new mineral species, crystal structure, Raman, Valletta, Piedmont, Italy.

Introduction

This is the second in a series of new-mineral descriptions of As-bearing minerals from Valletta mine (Cámara *et al*., 2014). The sample containing braccoite, the As-analogue of saneroite, was collected by one of the authors (MM) in 2012 in the dumps of Valletta mine, Vallone della Valletta, Canosio municipality, Maira Valley, Cuneo province, Piedmont, Italy (44º23′54″N, 7º5′42″E, 2562 m asl).

The name is in honour of Dr Roberto Bracco (b. 1959), a systematic minerals collector with a special interest in manganese minerals (Barresi *et al*., 2005; Bracco and Balestra, 2014). Dr Bracco has authored or coauthored several publications on systematic mineralogy, especially those devoted to new occurrences in Liguria (Bracco *et al*., 2006; 2012). The new mineral was approved by the International Mineralogical Association Commission on New Minerals, Nomenclature and Classification (IMA 2013-093).

A fragment of the holotype material has been deposited in the mineralogical collections of the Museo Regionale di Scienze Naturali di Torino, Sezione di Mineralogia, Petrografia e Geologia, Torino, Italy, catalogue number M/15939.

Braccoite is intergrown with tiragalloite, which is a rare mineral. For this reason the chemical and Raman spectrum of tiragalloite [$Mn_4^{2+}As^{5+}Si_3O_{12}(OH)$] from Valletta mine is also provided.

Geological setting and mineral occurrence

Brief geological and historical information was provided in Cámara *et al*. (2014). The deposit at Valletta mine has never been studied from a genetic point of view and available geological data for the area provide limited detail. Other than the historical texts, there is no mention in the literature of the occurrence of metalliferous mineralization in this locality. Preliminary work carried out during sampling showed that it is a small iron deposit with subordinate manganese, in quartzites with quartz veins that contain a large variety of mineral phases rich in arsenic, vanadium, barium and strontium. The volume of the mineralized body is, however, rather limited at the surface.

The rock hosting braccoite is compact, granular, dark red verging on black quartzite. Blocks of this material have been dug up and piled up in a small landfill where they have been mixed with calcareous rocks also from the excavated material.

Braccoite is strictly associated with tiragalloite, and with gamagarite, hematite, manganberzeliite, palenzonaite, quartz, saneroite, tokyoite, unidentified Mn oxides, organic compounds, and Mn arsenates and silicates under study. These findings make, in terms of mineralogical variety, the small dump of the old Valletta mine one of the richest Italian deposits of arsenate and silicoarsenate mineral phases, similar to those of Graveglia Valley (Antofilli *et al*. 1983; Borgo and Palenzona, 1988; Palenzona, 1991, 1996; Marchesini and Pagano, 2001). Other As-rich minerals found in the rock samples collected in the dump, although not strictly associated with braccoite are: adelite $CaMg(AsO_4)(OH)$, arseniopleite-caryinite series $(Ca,Na)NaMn^{2+}(Mn^{2+},Mg,Fe^{2+})_2(AsO_4)_3$–$(Na,Pb)(Ca,Na)CaMn_2^{2+}(AsO_4)_3$, bariopharmacosiderite $Ba_{0.5}Al_4(AsO_4)_3(OH)_4{\cdot}4H_2O$, berzeliite $NaCa_2Mg_2(AsO_4)_3$, grandaite $Sr_2Al(AsO_4)_2(OH)$ (IMA2013-059) and tilasite $CaMg(AsO_4)F$; these are found along with aegirine, albite, azurite, baryte, braunite, calcite, diopside, fluorapatite, ganophyllite, gypsum, ilmenite, hollandite, malachite, magnesio-arfvedsonite, magnesio-riebeckite, magnetite, mimetite, muscovite, neotocite, opal, orthoclase, phlogopite, ranciéite, richterite, rutile, rhodonite, talc, tetrahedrite, titanite and some other unknown phases under investigation.

Mineralogical characterization

Appearance and physical properties

Braccoite occurs as subhedral equant crystals, a few hundred microns across, with uneven fracture, grouped in thin masses, a few centimetres in size (Fig. 1), on granular red-brown quartzite with reddish-brownish-black K-feldspar and compact quartz. In rare cases the mineral forms rims around the remnants of protolithic quartz clasts. Individual crystals are brown-red in colour and translucent. Braccoite has a pale-yellow streak, a vitreous to resinous lustre and

https://doi.org/10.1180/minmag.2015.079.1.14 Published online by Cambridge University Press

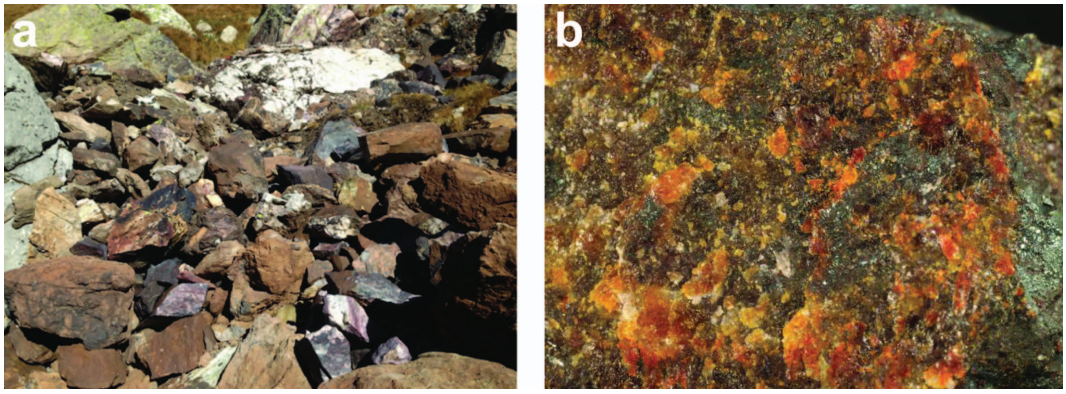

FIG. 1. (*a*) The rocks containing braccoite; (*b*) rare red crystalline masses with brown hue of braccoite holotype intergrown with orange tiragalloite forming a thin layer on hematite and quartz (field of view: 5 mm). Photo: R. Bracco.

does not fluoresce under shortwave or longwave ultraviolet light. Braccoite is optically biaxial positive, with a $2V_{meas}$ = 26(2)º and $2V_{calc}$ = 35º. The measured refractive indices are α = 1.749(1), β = 1.750(1) and γ = 1.760(1) (589 nm). Braccoite is weakly pleochroic with *X* = brownish yellow, *Y* = dark yellow, *Z* = yellow. The mineral is brittle and no cleavage or parting is observed. Hardness and density were not measured due to the small crystal size and because it occurs intimately intergrown with tiragalloite. The calculated density obtained from the empirical formula and unit-cell parameters of the single crystal used for the crystal-structure determination is 3.56 g/cm^3.

Chemical data

The chemical composition of braccoite was determined using a Cameca SX-50 electron microprobe (wavelength-dispersive spectroscopy mode, WDS) at the Department of Geosciences (Università di Padova) on a thin section obtained from the holotype close to the place where the crystal used for the diffraction study was extracted. Major and minor elements were determined at 20 kV accelerating voltage and 20 nA beam current (beam size 2 μm), with 40 to 20 s counting time on both peak and background. X-ray counts were converted to oxide wt.% using the '*PAP*' correction program supplied by Cameca (Pouchou and Pichoir, 1984; 1985). The crystals studied in the thin section (Fig. 2) were found to be homogeneous. Fe, Sb and Pb were analysed but were below detection limits. H_2O was calculated on the basis of 2OH groups per formula unit (p.f.u.) (Nagashima and Armbruster, 2010*a*). The averages of five analyses are given in Table 1*a*. Low totals are related to the difficulty with preparing good thin sections of polymineralic aggregates, and have also been reported for saneroite samples (Nagashima and Armbruster, 2010*a*).

The empirical formula, calculated on the basis of 19 O atoms per formula unit (a.p.f.u.) and considering 2(OH) is, within rounding errors, $Na_{1.06}(Mn^{2+}_{4.46}Mn^{3+}_{0.32}Mg_{0.19}Al_{0.01}Ca_{0.01})_{\Sigma 4.99}[(Si_{5.36}As_{0.48}V_{0.15})_{\Sigma 5.99}O_{17}(OH)](OH_{0.98}F_{0.02})$. Alternatively, the empirical formula, calculated on the basis of Σ cations − (Na,K) = 11, Mn^{2+}/Mn^{3+}ratio calculated in order to obtain [2(OH) − (Na−0.5)] groups p.f.u. [Mn^{3+}/(total Mn) = 0.066] and tetrahedral V^{5+} calculated as 6 − (Si+As), and with excess V assigned to the

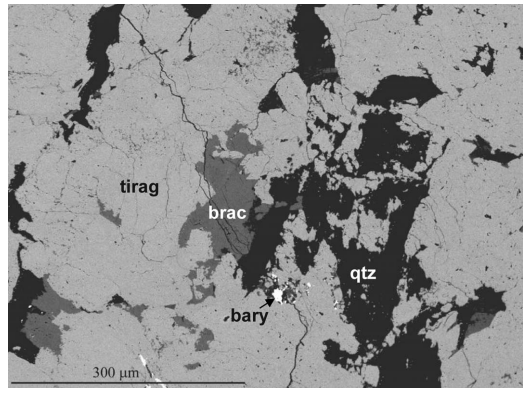

FIG. 2. Backscattered electron image of a section of a quartz (qtz) vein showing braccoite (brac) and tiragalloite (tirag) used during the WDS analyses. The small spot within quartz is baryte (bary).

https://doi.org/10.1180/minmag.2015.079.1.14 Published online by Cambridge University Press

TABLE 1*a*. Chemical data for braccoite (five analytical points).

	Wt.%	Range	SD	Probe standard (line)
Na_2O	4.06	3.72–4.22	0.20	albite Amelia (Na$K\alpha$)
CaO	0.05	0.03–0.06	0.01	diopside (Ca$K\alpha$)
MgO	0.96	0.90–1.01	0.05	synthetic periclase (Mg$K\alpha$)
MnO	41.76	40.94–42.46	0.41	$MnTiO_3$ (Mn$K\alpha$)
Mn_2O_3***	3.07	2.55–3.87	0.53	
Al_2O_3	0.04	0.01–0.12	0.04	corundum (Al$K\alpha$)
CuO	0.02	0.01–0.04	0.01	metallic Cu (Cu$K\alpha$)
SiO_2	39.73	38.70–40.21	0.59	diopside (Si$K\alpha$)
As_2O_5	6.87	6.10–7.79	0.61	synthetic AsGa (As$L\alpha$)
V_2O_5**	1.43	1.35–1.61	0.11	vanadinite (V$K\alpha$)
SO_3	0.01	0.01–0.02	0.01	sphalerite (S$K\alpha$)
F	0.04	0.00–0.19	0.00	fluorite (F$K\alpha$)
H_2O*	2.20	2.12–2.24		
O = F	−0.02	0.08–0.00		
Total	97.44	96.85–98.26		

* H_2O calculated in order to have 2(OH) p.f.u.
** total V is reported as V_2O_5 but tetrahedral V^{5+} is calculated as 6 − (Si + As) and excess V is assigned to the octahedral sites as V^{3+}, following Nagashima and Ambruster (2010*a*)
*** Mn^{2+}/Mn^{3+} ratio calculated (Mn^{3+}/total Mn = 0.066) in order to obtain 2(OH) groups p.f.u. and V distributed as reported.

Table 1*b*. Comparison of chemical data available for tiragalloite from other localities.

Wt.%	Valletta mine, Italy (1)	Molinello mine, Italy (2)	Ködnitz Valley, Austria (3)
As_2O_5	16.91	16.07	18.35
V_2O_5	0.59	1.67	
Sb_2O_5	0.01		
SiO_2	31.45	32.38	31.91
TiO_2			0.02
Al_2O_3			0.02
FeO	–	0.17	0.56
MnO	46.88	48.34	46.02
CaO	0.27	0.75	0.75
MgO	0.39	–	0.00
PbO	0.04		
SO_3	0.03	–	
Na_2O	0.01		0.03
F	0.11		
O=F	0.05		
Total	96.59	99.38	97.66

(1) This work (average of three analytical points); (2) Gramaccioli *et al*. (1980); (3) Albrecht (1990).

octahedral sites as V^{3+}, following Nagashima and Armbruster (2010*a*), within rounding errors, is $Na_{1.06}(Mn^{2+}_{4.46}Mn^{3+}_{0.32}Mg_{0.19}V^{3+}_{0.01}Al_{0.01}Ca_{0.01})_{\Sigma=5.00}$ $[Si_{5.37}As^{5+}_{0.48}V^{5+}_{0.15}O_{17}(OH)](OH_{0.98}F_{0.01})$. The simplified formula can be written as: $NaMn^{2+}_5[Si_5AsO_{17}(OH)](OH)$, which requires

https://doi.org/10.1180/minmag.2015.079.1.14 Published online by Cambridge University Press

Na_2O 3.78, MnO 43.31, SiO_2 36.68, As_2O_5 14.03 and H_2O 2.20, total 100 wt.%. The presence of OH was confirmed by micro-Raman spectroscopy. The mean refractive index *n* of braccoite, the calculated density and the empirical formula yielded a Gladstone-Dale compatibility index (Mandarino 1979, 1981) of 0.020, rated as excellent. Braccoite is unreactive and insoluble in 2 M and 10% HCl and 65% HNO_3.

The chemical data of tiragalloite [$Mn_4^{2+}As^{5+}Si_3O_{12}(OH)$] from Valletta mine and tiragalloite from the type-locality of Molinello mine (Ne, Graveglia Valley, Liguria, Italy) reported by Gramaccioli *et al*. (1980) are compared in Table 1*b*. Considering a stoichiometric H_2O content in order to have one (OH) group p.f.u., i.e. 1.46 wt.% H_2O, and 13 oxygen a.p.f.u., the formula corresponding to the average of three analyses is $(Mn^{2+}_{3.92}Mg_{0.06}Na_{0.03})_{\Sigma 4.01}(As^{5+}_{0.87}V^{5+}_{0.05}Si^{4+}_{0.09})_{\Sigma 1.01}Si_3O_{12}(OH_{0.96}F_{0.04})$.

Micro-Raman spectroscopy

The Raman spectrum of braccoite (Fig. 3) was obtained at the Dipartimento di Scienze della Terra (Università di Torino) using a micro/macro Jobin Yvon LabRam HRVIS, equipped with a motorized x–y stage and an Olympus microscope. The backscattered Raman signal was collected with 50× objective and the spectrum was obtained for a non-oriented crystal. The 632.8 nm line of an He-Ne laser was used as excitation; laser power (20 mW) was controlled by means of a series of density filters. The minimum lateral and depth resolution was set to a few μm. The 532 nm line of a Nd laser was also used as excitation; laser power (80 mW) was dosed by means of a series of density filters. An aperture of 200 μm was used to reduce the beam dose. The lateral and depth resolution were ~2 and 5 μm, respectively. The system was calibrated using the 520.6 cm^{-1} Raman band of silicon before each experimental session. Spectra were collected with multiple acquisitions (2 to 6) with single counting times ranging between 20 and 180 s. The spectrum was recorded using the *LabSpec 5* software package (Horiba Jobin Yvon, 2004, 2005) from 200 to 4000 cm^{-1}. Spectra collected with both lasers were equivalent. The spectrum reported in Fig. 3 was collected with the 632.8 nm line of the He-Ne laser.

There is a close match between the braccoite spectrum and that of saneroite from the type locality of Molinello mine (Graveglia Valley, Liguria, Italy) in the RRUFF database (R060488) (Downs, 2006). All the bands observed between 700 and 1000 cm^{-1} are characteristic of the two groups present in braccoite, SiO_4^{4-} and $AsO_3(OH)^{2-}$ (Myneni *et al.*, 1998*a*,*b*; Nakamoto, 1986). The spectrum shows intense bands at ~829, 907 and 932 (823, 909 and 936 cm^{-1} for saneroite R060488 in the RRUFF database, respectively, and weak peaks at 706 and 748 cm^{-1} (700 and 729 cm^{-1} for saneroite

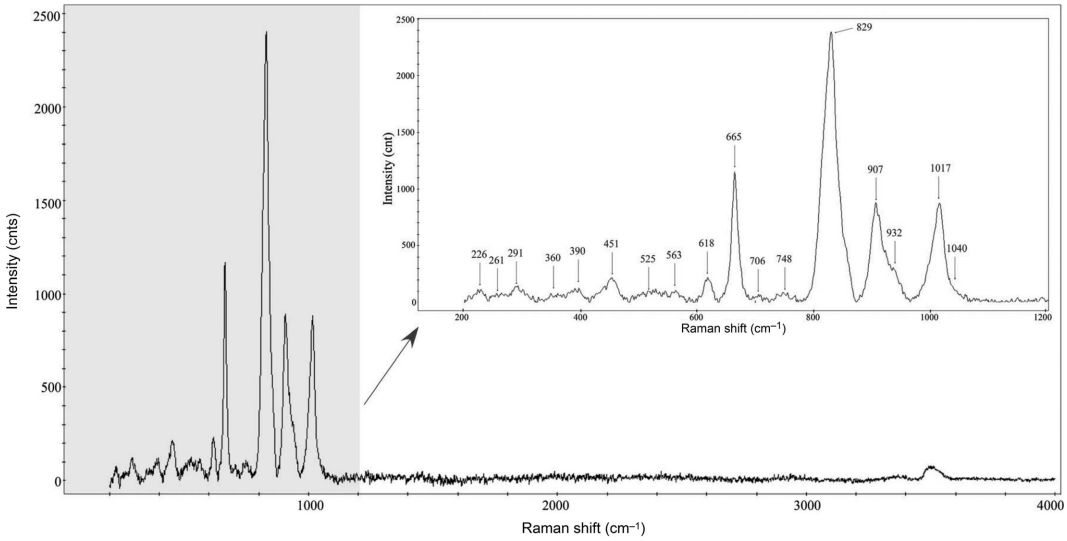

FIG. 3. Raman spectra of braccoite in the 200−4000 cm^{-1} region and (inset) between 200 and 1200 cm^{-1}.

https://doi.org/10.1180/minmag.2015.079.1.14 Published online by Cambridge University Press

R060488). The intense peak at 1017 cm^{-1} with a weak shoulder at 1040 cm^{-1} may be assigned to the ν_1 symmetric stretching mode of the SiO_4 units (Mills *et al*., 2005) (1011 and 1022 cm^{-1} for saneroite R060488) while the region assigned in the pyroxenes to the stretching modes of the Si–O bonds is present in the braccoite spectrum at 665 cm^{-1} (660 cm^{-1} for saneroite R060488). Bending modes of O–Si–O are observed at 525 cm^{-1} and 563 cm^{-1} for braccoite, while the Raman spectrum of saneroite R060488 shows a single weak band around 523 cm^{-1}. Cation–oxygen vibration modes appear in the low region of the spectrum below 460 cm^{-1}: weak and broad peaks are observed at 226, 261, 291, 360, 390 and 451 cm^{-1} (228, 281, 343, 376 and 436 cm^{-1} for saneroite R060488, respectively). The Raman spectrum of braccoite shows a broad envelope of overlapping bands centred upon 3361 and 3507 cm^{-1}, which are characteristic of OH stretching modes, in accordance with the presence of hydroxyl groups in the structure (the spectrum of saneroite R060488 was only collected for <1200 cm^{-1}).

Tiragalloite is intergrown with braccoite in rocks from Valletta mine. There is no available Raman spectrum for tiragalloite and therefore a spectrum was also collected for this mineral phase (Fig. 4). The spectrum shows a strong absorption centred at 869 cm^{-1} with three shoulders at 803, 836 and 902 cm^{-1}, two intense peaks at 661 and 647 cm^{-1}, weaker peaks at 960, 975 cm^{-1}, and a broad band at ~1004 cm^{-1}. As for braccoite and saneroite, the frequency separations between the bands due to the asymmetric and the symmetric stretches of the anionic groups $(SiO_4)^{4-}$ and $(AsO_4)^{3-}$ in tiragalloite vary strongly from one structure to another, and cannot be assigned with conviction (Hawthorne *et al*., 2013). Bands with frequencies between 250 and 600 cm^{-1} correspond to $(SiO_4)^{4-}$ and $(AsO_4)^{3-}$ vibrations (286, 320, 364, 398, 481, 508 and 549 cm^{-1}), while weak and broad bands <250 cm^{-1} correspond to lattice modes (153, 181 and 218 cm^{-1}). In the region between 1200 and 3000 cm^{-1} the spectrum displays a considerable amount of noise (a broad envelope of overlapping bands centred upon 1635, 1702 and 1799 cm^{-1}); this is a result of the low intensity of the bands. In accordance with the presence of hydroxyl groups in the structure, a wide and weak band was found at ~3100 cm^{-1}. Based on the Libowitzky (1999) correlation, the band at ~3100 cm^{-1} can be possibly assigned to the O11–*H*(11)···O1 bond present in tiragalloite (O11···O1 = 2.725 Å corresponding to 3257 cm^{-1}, using crystal data provided by Nagashima and Armbruster 2010*b*).

X-ray diffraction (XRD)

The powder XRD pattern of braccoite was obtained at CrisDi (Interdepartmental Center for Crystallography, Torino, Italy) using an Oxford Gemini R Ultra diffractometer equipped with a

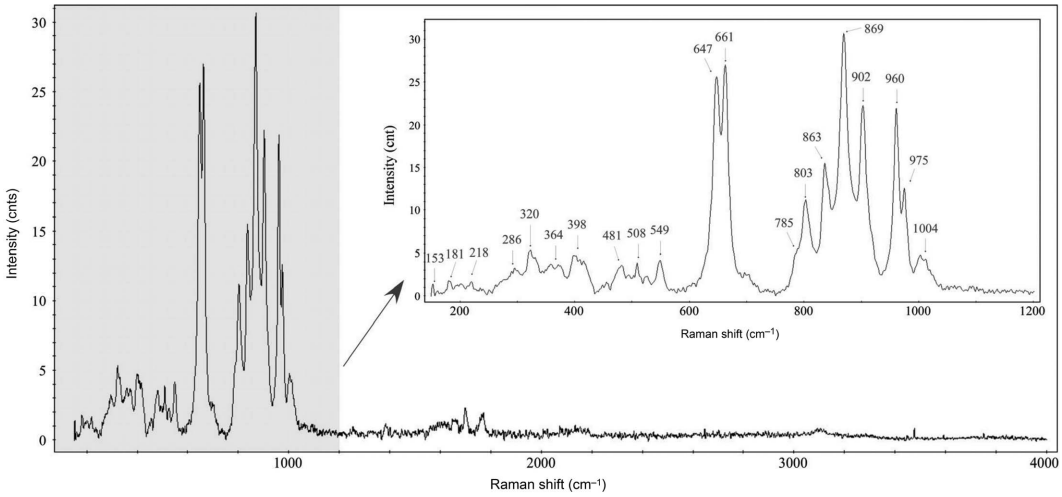

FIG. 4. Raman spectra of tiragalloite in the 150–4000 cm^{-1} region and (inset) between 150 and 1200 cm^{-1}.

https://doi.org/10.1180/minmag.2015.079.1.14 Published online by Cambridge University Press

CCD area detector, with graphite-monochromatized Mo$K\alpha$ radiation. Indexing of the reflections was based on a calculated powder pattern obtained from the structural model, using the software *LAZY PULVERIX* (Yvon *et al.*, 1977). Experimental and calculated data are reported in Table 2. The unit-cell parameters refined from the powder data with the software *GSAS* (Larson and Von Dreele, 1994) are a = 9.756(6), b = 9.961(7), c = 9.087(7) Å, α = 92.23(5), β = 117.27(5), γ = 105.21(4)º, V = 742.2(9) Å^3.

Single-crystal XRD data were collected using an Oxford Gemini R Ultra diffractometer equipped with a CCD area detector at CrisDi with graphite-monochromatized Mo$K\alpha$ radiation (λ = 0.71073 Å). A crystal fragment showing sharp optical extinction behaviour was used for collecting intensity data. No crystal twinning was observed. Crystal data and experimental details are reported in Table 3. The intensities of 7946 reflections with $-13 < h < 14$, $-14 < k < 14$, $-13 < l < 13$ were collected to 64.4º2θ using a 1º frame and an integration time of 20 s. Data were integrated and corrected for Lorentz and polarization background effects, using the package *CrysAlisPro* (Agilent Technologies, Version 1.171.36.20, release 27-06-2012 CrysAlis171.36.24). Data were corrected for empirical absorption using spherical harmonics, implemented in the *SCALE3 ABSPACK* scaling algorithm in *CrysAlisPro*. Refinement of the unit-cell parameters was based on 4389 measured reflections with $I > 10\sigma(I)$. At room temperature, the unit-cell parameters are a = 9.7354(4), b = 9.9572(3), c = 9.0657(3) Å, α = 92.691(2), β = 117.057(4), γ = 105.323(3)º, V = 740.37(4) Å^3,

TABLE 2. Observed and calculated powder XRD data for braccoite. The ten strongest reflections are reported in bold*.

h	k	l	d_{obs} (Å)	d_{calc} (Å)	Int.$_{(obs)}$	Int.$_{(calc)}$	h	k	l	d_{obs} (Å)	d_{calc} (Å)	Int.$_{(obs)}$	Int.$_{(calc)}$
1	$\bar{1}$	1	4.785	4.798	8	7.8	2	$\bar{2}$	2	2.393	2.399	9	2.3
0	2	0	4.723	4.710	8	10.2	0	4	$\bar{1}$	2.388	2.388	22	6.1
2	$\bar{2}$	$\bar{1}$	3.850	3.842	7	6.1	**4**	**$\bar{1}$**	**$\bar{1}$**	**2.381**	**2.378**	**58**	**18.7**
2	$\bar{1}$	$\bar{2}$	3.836	3.820	21	7.6	0	4	0	2.361	2.355	11	2.9
1	1	1	3.785	3.767	7	6.5	2	2	1	2.283	2.271	12	14.8
0	2	1	3.763	3.741	16	14.7	**2**	**1**	**$\bar{4}$**	**2.226**	**2.224**	**25**	**13.6**
2	$\bar{2}$	0	3.741	3.748	9	7.3	0	4	$\bar{2}$	2.218	2.223	20	11.3
2	1	$\bar{2}$	3.522	3.516	8	1.6	3	$\bar{4}$	$\bar{1}$	2.204	2.202	21	24.8
0	1	2	3.438	3.420	10	1.1	1	0	$\bar{4}$	2.186	2.181	6	4.1
1	2	$\bar{2}$	3.337	3.341	19	10.0	2	$\bar{3}$	$\bar{3}$	2.185	2.172	8	4.5
1	$\bar{3}$	0	3.310	3.308	8	8.1	3	$\bar{4}$	$\bar{2}$	2.091	2.084	9	5.5
1	$\bar{2}$	$\bar{2}$	3.212	3.192	9	3.5	1	2	$\bar{4}$	2.082	2.084	10	14.1
1	$\bar{1}$	2	3.143	3.147	19	27.2	3	1	1	2.067	2.060	12	13.9
1	$\bar{3}$	$\bar{1}$	3.055	3.042	6	2.4	5	$\bar{1}$	$\bar{4}$	1.779	1.773	7	6.5
2	**$\bar{2}$**	**1**	**3.055**	**3.064**	**69**	**55.4**	3	1	2	1.738	1.732	7	7.0
1	$\bar{3}$	1	3.054	3.063	17	18.2	1	2	$\bar{5}$	1.693	1.694	9	5.5
1	**0**	**2**	**3.042**	**3.037**	**43**	**15.2**	4	$\bar{5}$	0	1.680	1.683	24	15.3
3	**$\bar{2}$**	**$\bar{1}$**	**3.012**	**3.010**	**65**	**26.9**	**4**	**3**	**$\bar{3}$**	**1.680**	**1.676**	**36**	**25.9**
2	$\bar{3}$	0	2.998	3.002	6	4.7	4	$\bar{2}$	$\bar{5}$	1.655	1.648	14	14.7
2	**$\bar{3}$**	**$\bar{1}$**	**2.985**	**2.979**	**55**	**31.5**	3	$\bar{3}$	3	1.595	1.599	7	5.7
1	0	$\bar{3}$	2.974	2.967	8	4.7	0	5	2	1.595	1.586	13	13.7
2	**1**	**$\bar{3}$**	**2.825**	**2.822**	**100**	**100.0**	4	0	2	1.545	1.542	7	6.1
2	**2**	**0**	**2.708**	**2.696**	**92**	**72.7**	0	3	$\bar{5}$	1.537	1.540	6	5.1
1	1	2	2.699	2.687	6	10.0	5	$\bar{3}$	$\bar{5}$	1.495	1.488	9	7.8
1	3	0	2.673	2.661	20	10.8	3	$\bar{1}$	$\bar{6}$	1.485	1.480	7	2.9
3	0	$\bar{3}$	2.655	2.647	12	17.8	6	0	$\bar{5}$	1.440	1.436	6	2.4
2	**$\bar{3}$**	**$\bar{2}$**	**2.627**	**2.614**	**43**	**29.4**	1	0	5	1.434	1.431	15	13.2
0	1	3	2.433	2.422	15	18.1	6	$\bar{3}$	0	1.434	1.434	15	12.7

* Only reflections with $I_{rel} > 6\sigma(I_{rel})$ are listed; differences in observed and calculated intensities are related to preferred orientation.

https://doi.org/10.1180/minmag.2015.079.1.14 Published online by Cambridge University Press

TABLE 3. Crystal data and summary of parameters describing data collection and refinement for braccoite.

Crystal system	Triclinic
Space group	$P\bar{1}$
Unit-cell dimensions	
a (Å)	9.7354(4)
b (Å)	9.9572(3)
c (Å)	9.0657(3)
α (º)	92.691(2)
β (º)	117.057(4)
γ (º)	105.323(3)
V (Å^3)	740.37(4)
Z	2
μ (mm^{-1})	5.62
F(000)	758.78
D_{calc} (g cm^{-3})	3.56
Crystal size (mm)	0.20 × 0.15 × 0.17
Radiation type	Mo$K\alpha$ (0.71073 Å)
θ range for data collection (º)	3.5−32.3
R_{int} (%)	3.13
Reflections collected	18,039
Independent reflections	4911
$F_o > 4\sigma(F)$	4389
Refinement method	least-squares matrix: full
No. of refined parameters	300
Final R_{obs} (%) all data	4.14
R_1 (%) $F_o > 4\sigma(F)$	3.47
wR_2 (%) $F_o > 4\sigma(F)$	8.61
Highest peak/deepest hole (e$^-$ Å^{-3})	+0.81 / −0.66
Gof on F^2	1.191

space group $P\bar{1}$ and Z = 2. The a:b:c ratio is 0.978:1:0.910. A total of 4911 independent reflections were collected and the structure was solved and refined using the *SHELX* set of programs (Sheldrick, 2008).

Description of the structure

Structure model

The crystal structure of braccoite (Fig. 5) is topologically identical to that of the hydropyroxenoid saneroite. Both crystals have a five repeat single isolated chain of SiO_4 tetrahedra which have a sixth tetrahedron as an appendix. In this latter tetrahedron the $Si_{1-x}As_x$ substitution occurs ($Si_{1-x}V^{5+}_x$ in saneroite). Chains repeat laterally by a centre of symmetry forming a layer of tetrahedra parallel to $(1\bar{1}1)$. Five octahedral sites occupied by Mn (mostly Mn^{2+}, with some Mn^{3+}) form a band which runs parallel to two single chains of tetrahedra attached above and below. Laterally the bands are separated by channels occupied partially by two independent *Na* sites, one occupied completely and another with partial occupation. The structure of braccoite was therefore refined starting from the atom coordinates of saneroite excluding *H* sites (Nagashima and Armbruster, 2010*a*). The nomenclature of the sites therefore follows that of the aforementioned authors. Scattering curves for neutral and ionized atoms were taken from the *International Tables for Crystallography* (Wilson, 1992). Site-scattering values were refined for the cation sites using two scattering curves contributing proportionally and a constrained sum to full occupancy: Mn^{2+} and Mg were used for the sites *Mn*(1−5); Si^{4+} full occupancy was fixed at the *T*(1−5) sites, while Si^{4+} and As were used at the *T*(6) site; Na^+ was used for the *Na*(1) and *Na*(2) sites, although the occupancy was held fixed at *Na*(1) and refined at *Na*(2). After converging, the positions of two H atoms [*H*(7) and *H*(19) sites] were located in difference Fourier maps and added to the model; atom coordinates of *H* sites were refined and isotropic thermal parameters were constrained to be 1.2 times the isotropic equivalent of the

https://doi.org/10.1180/minmag.2015.079.1.14 Published online by Cambridge University Press

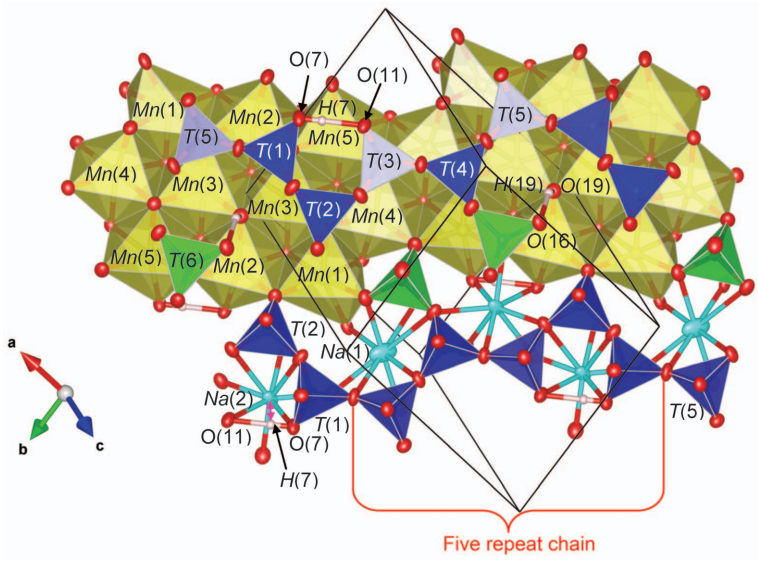

FIG. 5. Detail of the braccoite structure showing the bands of Mn octahedra and the silicate chains. Blue: Si tetrahedra; green: As−Si tetrahedron; yellow: Mn octahedra; light blue: Na; white: H. Violet double arrow shows the short *Na*(2)···*H*(7) distance. Approximate vector of projection is [5$\bar{1}$5]. Design obtained with *VESTA 3* (Momma and Izumi, 2011).

oxygen atom of the hydroxyl group assuming a riding motion model, while a soft constraint of 0.98 Å (Franks, 1973) was applied to the *H*(19)−O(19) distance. Structure refinement converged to R_1 = 0.0347 for 4389 reflections with $F_o > 4\sigma(F_o)$ and 0.0413 for all 4911 data. Tables 4, 5 and 6 report atomic coordinates, the displacement parameters and selected bond distances, and angles, respectively, for braccoite. Bond-valence calculations using the parameters of Brown (1981) are reported in Table 7. The cif and structure factor list files have been deposited with the Principal Editor of *Mineralogical Magazine* and are available from http://www.minersoc.org/pages/e_journals/dep_mat_mm.html.

Site occupancies

Cation sites

There are 13 cation sites in the braccoite structure: six sites are 4-coordinated, five sites are 6-coordinated and two are 8-coordinated. One of the six 4-coordinated sites, the *T*(6) site, has a larger mean atomic number [24.17(6) electrons per site (e.p.s.) *vs*. 14 e.p.s. for the other five sites, Table 4], and <T−O> is larger than that of the other five sites (1.675 Å *vs*. a mean of 1.624 Å for the other five sites, Table 6). Chemical analyses report the presence of both V^{5+} and As^{5+} that can order in a site with tetrahedral coordination. The refined site scattering is >23 e.p.s. and therefore implies dominance of As in the presence of sufficient amounts of Si. The latter is confirmed by electron microprobe (EMP) analyses (Table 1*a*). In the presence of a concomitant Si−V−As solid solution in a cation site with tetrahedral coordination, the size of the tetrahedron is not sufficient to provide the actual dominance of As^{5+} *vs*. V^{5+} because they have very similar ionic radii (0.335 and 0.355 Å, respectively, Shannon, 1976). The distances observed in the crystal studied (Table 6) are compatible with a Si−V substitution (values of 1.68−169 Å are usually found for saneroite, Nagashima and Armbruster, 2010*a*,*c*; 1.70 Å for medaite, Nagashima and Armbruster, 2010*b*). Note that, besides the chemical strain due to a three component solid solution, *T*(6) is not the most distorted 4-coordinated site in the structure. The *T*(5) site shows the greatest angle variance (σ^2 = 41.72, computed according to Robinson *et al*. 1971, Table 6) as observed for saneroite (σ^2 = 40.00, Basso and Della Giusta, 1980).

With regard to the five 6-coordinated sites, all are Mn^{2+} dominant. However, site *Mn*(3) is

https://doi.org/10.1180/minmag.2015.079.1.14 Published online by Cambridge University Press

TABLE 4. Multiplicities, fractional atom coordinates and equivalent isotropic displacement parameters (Å^2) for braccoite*.

	Site occupancy	*x/a*	*y/b*	*z/c*	U_{iso}
Na(1)	1 Na^+	½	0	½	0.0300(5)
Na(2)	0.521(6) Na^+	0.1912(3)	0.5340(2)	0.4432(3)	0.0151(7)
Mn(1)	0.953(5) Mn^{2+} 0.047(5) Mg^{2+}	0.74388(5)	0.97982(5)	0.29542(6)	0.01168(14)
Mn(2)	0.917(5) Mn^{2+} 0.083(5) Mg^{2+}	0.99723(5)	0.21282(5)	0.22004(6)	0.01045(15)
Mn(3)	0.843(5) Mn^{2+} 0.157(5) Mg^{2+}	0.86298(5)	0.88807(5)	0.02950(6)	0.00981(16)
Mn(4)	0.944(5) Mn^{2+} 0.056(5) Mg^{2+}	0.57398(5)	0.66844(4)	0.09774(5)	0.00999(15)
Mn(5)	0.953(5) Mn^{2+} 0.047(5) Mg^{2+}	0.71912(5)	0.55370(5)	0.85346(6)	0.01242(15)
T(1)	1 Si^{4+}	0.87449(9)	0.27556(8)	0.82439(10)	0.00920(15)
T(2)	1 Si^{4+}	0.03102(9)	0.23894(8)	0.60955(9)	0.00861(15)
T(3)	1 Si^{4+}	0.20746(9)	0.54939(8)	0.77372(10)	0.00943(15)
T(4)	1 Si^{4+}	0.47814(9)	0.75745(8)	0.73037(9)	0.00925(15)
T(5)	1 Si^{4+}	0.61959(9)	0.07757(8)	0.89560(9)	0.00829(15)
T(6)	0.465(3) Si^{4+} 0.535(3) As	0.60697(5)	0.71401(4)	0.48355(5)	0.00903(12)
O(1)	1 O	0.7048(2)	0.1654(2)	0.7947(3)	0.0132(4)
O(2)	1 O	0.8853(2)	0.2267(2)	0.6567(3)	0.0145(4)
O(3)	1 O	0.1110(2)	0.4094(2)	0.6204(3)	0.0133(4)
O(4)	1 O	0.3022(2)	0.6692(2)	0.7062(3)	0.0124(4)
O(5)	1 O	0.4987(2)	0.9265(2)	0.7529(3)	0.0128(4)
O(6)	1 O	0.4645(2)	0.7114(2)	0.5465(3)	0.0142(4)
O(7)	1 O	0.8556(3)	0.4331(2)	0.8222(3)	0.0144(4)
O(8)	1 O	0.9645(2)	0.7248(2)	0.0081(3)	0.0118(4)
O(9)	1 O	0.9535(2)	0.1532(2)	0.4220(2)	0.0123(4)
O(10)	1 O	0.8287(2)	0.8130(2)	0.2469(2)	0.0110(4)
O(11)	1 O	0.0805(2)	0.6058(2)	0.8035(3)	0.0143(4)
O(12)	1 O	0.6649(2)	0.4918(2)	0.0594(2)	0.0114(4)
O(13)	1 O	0.3746(2)	0.2765(2)	0.1181(2)	0.0113(4)
O(14)	1 O	0.4961(2)	0.1480(2)	0.9102(3)	0.0127(4)
O(15)	1 O	0.2404(2)	0.9490(2)	0.9367(2)	0.0112(4)
O(16)	1 O	0.6809(3)	0.8807(2)	0.4750(3)	0.0148(4)
O(17)	1 O	0.5172(2)	0.6042(2)	0.2977(3)	0.0137(4)
O(18)	1 O	0.2568(3)	0.3469(2)	0.3699(3)	0.0149(4)
O(19)	1 O	0.0897(2)	0.0502(2)	0.1728(3)	0.0134(4)
H(7)	1 H	0.937(5)	0.493(4)	0.820(5)	0.017***
H(19)**	1 H	0.179(3)	0.050(4)	0.276(3)	0.016***

* The temperature factor has the form $\exp(-T)$ where $T = 8\ (\pi^2)U(\sin(\theta)/\lambda)^2$ for isotropic atoms.
**Atom coordinates refined with a soft constraint to O–H = 0.98 Å.
***U_{iso} refined and constrained to be 1.2, the isotropic equivalent of the oxygen atom of the hydroxyl group.

significantly smaller (2.183 Å *vs*. 2.20–2.25 Å, Table 6). This can be interpreted as ordering of a lighter and smaller Mg cation, which is present in the chemical analyses. Yet ordering all the Mg at the *Mn*(3) site would require a site-scattering value smaller than that observed. On the other hand, a small quantity of Mn^{3+} has been inferred in the chemical formula (see Chemical data section) in order to achieve charge balance, assuming full occupancy of H at the *H*(7) and *H*(19) sites. In addition, Nagashima and Armbruster (2010*a*) confirmed the presence of a

https://doi.org/10.1180/minmag.2015.079.1.14 Published online by Cambridge University Press

TABLE 5. Anisotropic displacement parameters for braccoite (Å)*.

	U^{11}	U^{22}	U^{33}	U^{12}	U^{13}	U^{23}
Na(1)	0.0487(13)	0.0380(12)	0.0215(10)	0.0280(10)	0.0230(10)	0.0175(9)
Na(2)	0.0233(13)	0.0130(12)	0.0087(11)	0.0032(9)	0.0090(10)	0.0023(8)
Mn(1)	0.0098(2)	0.0107(2)	0.0128(2)	0.00149(16)	0.00516(17)	0.00090(16)
Mn(2)	0.0103(2)	0.0107(2)	0.0104(2)	0.00265(16)	0.00545(17)	0.00342(16)
Mn(3)	0.0098(2)	0.0093(2)	0.0112(2)	0.00304(17)	0.00566(18)	0.00310(16)
Mn(4)	0.0093(2)	0.0091(2)	0.0111(2)	0.00244(16)	0.00485(17)	0.00261(15)
Mn(5)	0.0125(2)	0.0113(2)	0.0153(2)	0.00397(17)	0.00813(18)	0.00284(16)
T(1)	0.0087(3)	0.0102(3)	0.0101(3)	0.0031(3)	0.0055(3)	0.0040(3)
T(2)	0.0085(3)	0.0092(3)	0.0079(3)	0.0025(3)	0.0039(3)	0.0027(3)
T(3)	0.0086(3)	0.0088(3)	0.0110(3)	0.0021(3)	0.0050(3)	0.0039(3)
T(4)	0.0097(3)	0.0090(3)	0.0093(3)	0.0025(3)	0.0049(3)	0.0038(3)
T(5)	0.0081(3)	0.0091(3)	0.0086(3)	0.0029(3)	0.0044(3)	0.0038(3)
T(6)	0.0098(2)	0.00979(19)	0.00859(19)	0.00275(14)	0.00542(15)	0.00280(13)
O(1)	0.0107(9)	0.0153(9)	0.0142(9)	0.0024(7)	0.0072(8)	0.0071(8)
O(2)	0.0118(9)	0.0220(10)	0.0113(9)	0.0053(8)	0.0069(8)	0.0043(8)
O(3)	0.0159(10)	0.0102(9)	0.0104(9)	0.0016(7)	0.0049(8)	0.0020(7)
O(4)	0.0112(9)	0.0131(9)	0.0129(9)	0.0020(7)	0.0065(7)	0.0052(7)
O(5)	0.0138(9)	0.0087(8)	0.0121(9)	0.0012(7)	0.0045(8)	0.0036(7)
O(6)	0.0129(9)	0.0199(10)	0.0099(9)	0.0037(8)	0.0064(8)	0.0032(8)
O(7)	0.0134(10)	0.0108(9)	0.0214(11)	0.0042(8)	0.0101(8)	0.0058(8)
O(8)	0.0112(9)	0.0132(9)	0.0112(9)	0.0056(7)	0.0046(7)	0.0034(7)
O(9)	0.0137(9)	0.0134(9)	0.0087(9)	0.0022(7)	0.0056(7)	0.0019(7)
O(10)	0.0107(9)	0.0121(9)	0.0091(9)	0.0040(7)	0.0036(7)	0.0023(7)
O(11)	0.0148(10)	0.0140(9)	0.0200(10)	0.0063(8)	0.0120(8)	0.0069(8)
O(12)	0.0115(9)	0.0114(9)	0.0103(9)	0.0035(7)	0.0044(7)	0.0038(7)
O(13)	0.0128(9)	0.0120(9)	0.0103(9)	0.0051(7)	0.0059(7)	0.0040(7)
O(14)	0.0128(9)	0.0140(9)	0.0142(9)	0.0062(7)	0.0078(8)	0.0047(7)
O(15)	0.0115(9)	0.0110(9)	0.0104(9)	0.0034(7)	0.0048(7)	0.0044(7)
O(16)	0.0175(10)	0.0130(9)	0.0136(10)	0.0031(8)	0.0081(8)	0.0048(8)
O(17)	0.0142(9)	0.0142(9)	0.0105(9)	0.0017(8)	0.0060(8)	0.0003(7)
O(18)	0.0133(9)	0.0159(10)	0.0165(10)	0.0068(8)	0.0066(8)	0.0069(8)
O(19)	0.0125(9)	0.0153(9)	0.0112(9)	0.0049(8)	0.0044(8)	0.0034(7)

* The temperature factor has the form $\exp(-T)$ where $T = 2\pi^2\Sigma_{ij}(h(i)h(j)U(i,j)a\times(i)a\times(j))$.

limited quantity of Mn^{3+} in saneroite from Molinello (Graveglia Valley, Italy) by using the ratio of the X-ray intensities of the Mn$L\beta$ and Mn$L\alpha$ lines after the method of Albee and Chodos (1970) and Kimura and Akasaka (1999). Therefore, a limited amount of Mn^{3+} ($0.066Mn^{3+}/Mn_{total}$) was also assumed for braccoite. Incidentally, other Mn^{3+} phases have been found at the Valletta mine (e.g. grandaite, Cámara *et al*., 2014) and all the Fe-bearing phases contain Fe^{3+} only. Because there is no large bond-valence contribution to the *Mn*(3) site (Table 7) it is probable that Mn^{3+} is also distributed in the other two smaller sites, *Mn*(2) and *Mn*(4). In the structure of braccoite there is also one octahedron that is slightly larger than the others, the *Mn*(1) site. It would appear that this site should host the very small amount of Ca reported in the analyses, although that amount is not enough to justify the observed size enlargement. However, Ca could also be distributed at the *Na*(1) or *Na*(2) sites. The *Mn*(1) site is also more distorted (σ^2 = 170.51, compared to values ranging between 55.18 and 86.77, Table 6). This is possibly due to the fact that the oxygen at O(16) acts as bond donor to the proton at *H*(19) and that it is the only octahedron that shares an edge with a tetrahedron, the *T*(5) site, which is also the most distorted tetrahedron. The O(5)–O(14) edge involves two anion sites with among the highest and the lowest bond-valence contribution, respectively (Table 7), and is also the shortest. Hence there is a possible

https://doi.org/10.1180/minmag.2015.079.1.14 Published online by Cambridge University Press

TABLE 6. Main interatomic distances (Å) and geometrical parameters for braccoite.

Na(1)–O(5) (×2)	2.444(2)	*Mn*(2)–O(11)	2.119(2)	*Mn*(5)–O(7)	2.108(2)	*T*(3)–O(11)	1.604(2)
–O(16) (×2)	2.451(2)	–O(9)	2.136(2)	–O(17)	2.159(2)	–O(12)	1.618(2)
–O(1) (×2)	2.613(2)	–O(19)	2.161(2)	–O(13)	2.178(2)	–O(4)	1.628(2)
–O(6) (×2)	2.877(2)	–O(15)	2.189(2)	–O(12)	2.231(2)	–O(3)	1.642(2)
<*Na*(1)–O>	2.596	–O(18)	2.222(2)	–O(8)	2.270(2)	<*T*(3)–O>	1.623
**V (Å^3)	26.007	–O(8)	2.346(2)	–O(18)	2.374(2)	*V* (Å^3)	2.188
		<*Mn*(2)–O>	2.196	<*Mn*(5)–O>	2.220	σ^2*	7.846
Na(2)–O(18)	2.285(3)	*V* (Å^3)	13.711	*V*(Å^3)	14.066	λ*	1.0019
–O(4)	2.292(3)	σ^2*	67.545	σ^2*	86.772		
–O(7)	2.293(3)	λ*	1.0207	λ*	1.0260	*T*(4)–O(13)	1.602(2)
–O(3)	2.355(3)					–O(4)	1.612(2)
–O(6)	2.484(3)	*Mn*(3)–O(19)	2.116(2)	*T*(1)–O(8)	1.613(2)	–O(5)	1.633(2)
–O(11)	2.513(3)	–O(8)	2.156(2)	–O(1)	1.617(2)	–O(6)	1.643(2)
–O(2)	2.753(3)	–O(19)	2.163(2)	–O(7)	1.626(2)	<*T*(4)–O>	1.623
–O(3)	2.944(3)	–O(13)	2.191(2)	–O(2)	1.632(2)	*V* (Å^3)	2.181
<*Na*(2)–O>	2.490	–O(15)	2.199(2)	*T*(1)–O>	1.622	σ^2*	14.064
V (Å^3)	25.210	–O(10)	2.272(2)	*V* (Å^3)	2.178	λ*	1.0033
		<*Mn*(3)–O>	2.183	σ^2*	15.761		
Mn(1)–O(9)	2.069(2)	*V* (Å^3)	13.523	λ*	1.0038	*T*(5)–O(14)	1.592(2)
–O(10)	2.150(2)	σ^2*	55.177			–O(15)	1.607(2)
–O(16)	2.177(2)	λ*	1.0174	*T*(2)–O(9)	1.596(2)	–O(1)	1.634(2)
–O(14)	2.190(2)			–O(10)	1.626(2)	–O(5)	1.679(2)
–O(15)	2.308(2)	*Mn*(4)–O(14)	2.107(2)	–O(2)	1.635(2)	<*T*(5)–O>	1.628
–O(5)	2.627(2)	–O(12)	2.190(2)	–O(3)	1.647(2)	*V* (Å^3)	2.183
<*Mn*(1)–O>	2.253	–O(17)	2.199(2)	<*T*(2)–O>	1.626	σ^2*	41.722
V (Å^3)	14.087	–O(10)	2.220(2)	*V* (Å^3)	2.200	λ*	1.0098
σ^2*	170.515	–O(12)	2.246(2)	σ^2*	9.140		
λ*	1.0617	–O(13)	2.287(2)	λ*	1.0021		
		<*Mn*(4)–O>	2.208				
		V (Å^3)	13.939				
		σ^2*	67.478				
		λ*	1.0204				

T(6)–O(16)	1.646(2)		
–O(17)	1.667(2)		
–O(18)	1.670(2)		
–O(6)	1.719(2)		
<*T*(6)–O>	1.675		
V (Å^3)	2.403		
σ^2*	12.945		
λ*	1.0032		
		H(7)–O(7)	0.86(4)
		H(7)···O(11)	1.62(4)
		O(7)···O(11)	2.48(1)
		O(7)–*H*(7) ···O(11)	176.37(2)°
		H(19)–O(19)	0.95(2)
		H(19)···O(16)	1.99(2)
		O(19)···O(16)	2.855(10)
		O(19)–*H*(19)...O(16)	150.34(18)°

* Mean quadratic elongation (λ) and the angle variance (σ^2) were computed according to Robinson *et al.* (1971); ** V = polyhedral volume.

TABLE 7. Bond-valence calculations for braccoite (Brown, 1981).

	T(1)	*T*(2)	*T*(3)	*T*(4)	*T*(5)	*T*(6)	*M*(1)	*M*(2)	*M*(3)	*M*(4)	*M*(5)	*Na*(1)	*Na*(2)	*H*(7)	*H*(19)		+ H contrib.
O(1)	1.013				0.968							0.115 ×2↓				2.096	
O(2)	0.975	0.965											0.047			1.987	
O(3)		0.937	0.949										0.116 0.030			2.032	
O(4)			0.985	1.026									0.134			2.145	
[IV]O(5)				0.972	0.863		0.120					0.169 ×2↓				2.123	
[IV]O(6)				0.946		1.029						0.063 ×2↓	0.086			2.124	
[IV]O(7)	0.988										0.409		0.133	1.019 0.475		1.531	2.550 2.006
[IV]O(8)	1.024							0.223	0.353		0.271					1.871	
O(9)		1.073					0.457	0.376								1.906	
[IV]O(10)		0.988					0.369		0.264	0.306						1.928	
[IV]O(11)			1.050					0.393					0.081	0.255 0.475		1.524	1.779 1.999
O(12)			1.010							0.331 0.287	0.298					1.927	
[IV]O(13)				1.056					0.323	0.260	0.341					1.980	
O(14)					1.084		0.332			0.410						1.826	
[IV]O(15)					1.041		0.248	0.328	0.317							1.934	
[IV]O(16)						1.240	0.344					0.166 ×2↓			0.162	1.749	1.911
O(17)						1.173				0.323	0.358					1.855	
[IV]O(18)						1.167		0.302			0.211		0.136			1.815	
O(19)								0.353	0.392 0.347						0.824	1.091	1.915
	4.000	3.963	3.994	3.999	3.956	4.609	1.870	1.975	1.996	1.917	1.888	1.026	0.763	1.274 0.950	0.986		37.38
F.C.*	4.000	4.000	4.000	4.000	4.000	4.630	2.000	2.070	2.240	2.030	2.000	1.000	0.560	1.000	1.000	37.96	

Anion sites coordination reported only for coordination other than 3. *F.C: = formal charge at site on the basis of chemical formula.

charge-shielding mechanism operated by the electronic clouds of both oxygen atoms.

The 8-coordinated sites host Na atoms. The *Na*(1) site has full occupancy and bond distances are compatible with 1 a.p.f.u. of Na (Table 8), while the *Na*(2) site shows a refined site scattering which indicates approximately half occupancy of Na (Table 4). This site shares four edges with four Si tetrahedra and two edges with two Mn octahedra [*Mn*(2) and *Mn*(5)]. This is probably impeding the full occupancy of this site and produces a rather distorted bonding environment.

Taking into consideration the observed site-scattering values and those obtained from EMP analyses, the agreement for all cations sites is within 2% relative error, with slightly lighter values from diffraction data than obtained from chemical analyses (230.8 electrons per formula unit, e.p.f.u., *vs*. 233.9 e.p.f.u., respectively). Site-distribution according to the structure refinement (site scattering and bond distances) and electron microprobe data results give full occupancy of Si at the *T*(1−5) sites, *T*6 ($As^{5+}_{0.48}Si_{0.37}V^{5+}_{0.15}$), *Mn*1 ($Mn^{2+}_{0.98}Mg_{0.01}Ca_{0.01}$), *Mn*2 ($Mn^{2+}_{0.87}Mn^{3+}_{0.07}Mg_{0.06}$), *Mn*3 ($Mn^{2+}_{0.66}Mn^{3+}_{0.22}V^{3+}_{0.01}Al_{0.01}Mg_{0.10}$), *Mn*4 ($Mn^{2+}_{0.96}Mn^{3+}_{0.03}Mg_{0.01}$), *Mn*5 ($Mn^{2+}_{0.99}Mg_{0.01}$), *Na*1 ($Na_{1.00}$) and *Na*2 ($Na_{0.56}$), with an overall positive charge of 36.53. The agreement between observed values and those calculated from chemical composition after site assignment is reported in Table 8.

Anion sites

There are 19 anion sites in the structure of braccoite, ten are 3-coordinated and the rest are 4-coordinated (Table 7). There are three anion sites with a bond-valence incidence significantly greater than 2 vu: O(4), O(5) and O(6). The same atoms show also high bond-valence incidence for saneroite (Basso and Della Giusta, 1980; Nagashima and Armbruster, 2010*a*), in particular O(4), which is 3-coordinated; at the O(4) site, the contribution from *T*(3) and *T*(4) is already 2.011 vu and therefore the contribution from the *Na*(2) site (0.134 vu, Table 7) over-saturates this anion site. This is in fact another strong restriction preventing full occupancy of the *Na*(2) site (see above).

Two anion sites are actually 3-coordinated [O(11) and O(16)] but act as donors of two respective H bonds at O(7) and O(19). Chemical analyses show a very limited amount of fluorine. While it is not possible to assess in which site the fluorine orders, it is highly probable that it orders at the O(19) site: this site receives a bond-valence contribution of 1.091 vu (Table 7) and therefore hosts an (OH) group, which belongs to three octahedra of two *Mn*(3) and one *Mn*(2) site. The Raman spectrum in Fig. 3 shows a broad envelope of overlapping bands centred upon 3361 and 3507 cm^{-1}, which reflect the two essential next-neighbour configurations:

TABLE 8. Refined site-scattering and assigned site-populations for braccoite.

Site	Refined site-scattering (e.p.f.u.)	Assigned site-population (a.p.f.u.)	Calculated site-scattering (e.p.f.u.)	$\langle X-\varphi\rangle_{calc.}$* (Å)	$\langle X-\varphi\rangle_{obs.}$ (Å)	Ideal composition (a.p.f.u.)
		Cations				
Mn(1)	24.39(7)	0.98 Mn^{2+} + 0.01 Mg + 0.01 Ca	24.82	2.191	2.253	Mn^{2+}
Mn(2)	23.93(7)	0.87 Mn^{2+} + 0.07 Mn^{3+} + 0.06 Mg	24.22	2.170	2.196	Mn^{2+}
Mn(3)	22.96(7)	0.56 Mn^{2+} + 0.32 Mn^{3+} + 0.10 Mg + 0.01 V^{3+} + 0.01 Al^{3+}	23.53	2.130	2.183	Mn^{2+}
Mn(4)	24.28(7)	0.96 Mn^{2+} + 0.03 Mn^{3+} + 0.01 Mg	24.87	2.183	2.208	Mn^{2+}
Mn(5)	24.39(7)	0.99 Mn^{2+} + 0.01 Mg	24.87	2.189	2.220	Mn^{2+}
T(6)	24.17(6)	0.48 As + 0.37 Si + 0.15 V^{5+}	24.47	1.671	1.675	As
Na(1)	11.00	1.00 Na	11.00	2.560	2.596	Na**
Na(2)	5.72(6)	0.56 Na + 0.44 □	6.16	2.560	2.490	Na,o
		Anions				
$^{[IV]}$O(19)		0.98 OH + 0.02 F				OH

X = cation, φ = O, OH, F
* calculated by summing constituent ionic radii; values from Shannon (1976)
** site in special position, half multiplicity.

https://doi.org/10.1180/minmag.2015.079.1.14 Published online by Cambridge University Press

$Mn^{2+}Mn^{2+}Mn^{2+}$ and $Mn^{3+}Mn^{3+}Mn^{2+}$, while other configurations are also possible, i.e. $MgMgMn^{2+}$, $Mn^{3+}Mn^{3+}Mn^{3+}$ or even MgMgMg, yielding overall a broad band. Hydrogen bonding is also present at the O(7) anion site. However, in this case, a short distance with another oxygen atom at the O(11) anion site (2.48 Å) along with a similar bond-valence contribution, of 1.531 for O(7) and 1.524 valence units (vu) for O(11), is probably responsible for a very strong H bond (see later).

Hydrogen bonding

Strong H bonding is present in the braccoite structure as also observed in saneroite. A close inspection of Table 7 shows that there are four oxygen sites with bond-valence incidence <1.8 vu: O(7), O(11), O(16) and O(19). There is one very short acceptor–donor distance corresponding to a very strong H bond [O(7)···O(11) = 2.48 Å, Table 6], and another longer distance corresponding to a medium-strength H bond (O(19)···O(16) = 2.855 Å, Table 6). Using the relation $\nu\ (cm^{-1}) = 3592 - 304 \times 10^{9} \cdot \exp(-d(O\cdots O)/0.1321)$ (Libowitzky, 1999), bands should be expected at 1456 and 3467 cm^{-1}. While frequencies at ~3500 cm^{-1} are observed in the Raman spectrum of braccoite (Fig. 3) the expected band around 1400 cm^{-1} is not visible in the spectrum. The positions of two H atoms were observed in the Fourier-difference maps at convergence and were added to the model. In particular, the position observed for the *H*(7) atom shows a bond with oxygen at the O(7) anion site with a short *H*(7)···O(11) distance of 1.62(4) Å. The position of the corresponding H atom in saneroite was not detected by Basso and Della Giusta (1980) but was found with very similar atom coordinates by Nagashima and Armbruster (2010*a*) (x = 0.937(5) y = 0.493(4) z = 0.820(5) for braccoite and x = 0.940(3) y = 0.506(3) z = 0.815(4) for saneroite specimen 1 of Nagashima and Armbruster, 2010*a*, table 3), and a band at ~1400 cm^{-1} was observed in the Fourier transform infrared spectrum (FT-IR) collected on saneroite from Molinello by Brugger *et al*. (2006). The fact that both O(7) and O(11) show an equivalent bond-valence contribution (Table 7), suggests a plausible disordered environment for this proton. Such a situation, with a disordered position for H, has been observed in another related pyroxenoid structure, serandite ($NaMn_2[Si_3O_8(OH)]$), which shows an O···O distance of 2.464–2.468 Å (Jacobsen *et al*., 2000) and for which the IR O–H stretching mode was found at 1386 cm^{-1} (Hammer *et al*., 1998). Another topologically related structure is scheuchzerite ($NaMn_9^{2+}[Si_9V^{5+}O_{28}(OH)](OH)_3$; Brugger *et al*., 2006), which also has a very strong H bond among O(26) and O(29) anion sites, at a distance of 2.35 Å (Brugger *et al*., 2006). In this case a band is observed at 1466 cm^{-1} in the FTIR spectrum, which can correspond to the strong H bond. It should also be taken into account that the *H*(7) site is at a distance of 2.09(5) Å from the *Na*(2) site, which is not far of the Na–H distance in NaH (1.913 Å; Chen *et al*., 2005) and this surely stresses the bonding environment of the proton at around half of the *H*(7) sites.

Related minerals

Braccoite, $NaMn_5^{2+}[Si_5AsO_{17}(OH)](OH)$, is the As-dominant analogue of saneroite, $NaMn_5^{2+}[Si_5V^{5+}O_{17}(OH)](OH)$ (Basso and Della Giusta, 1980; Lucchetti *et al*., 1981; Nagashima and Armbruster, 2010*a*). For the dominant cation in the *T*6 site Nagashima and Armbruster (2010*a*) proposed adding a suffix, i.e. "saneroite-(V)", "saneroite-(Si)" and "saneroite-(As)". In the recent IMA guidelines, Hatert *et al*. (2013) have allowed the use of any other name confirming that "mineral names are chosen by the authors of new mineral species, according to guidelines established by Nickel & Grice (1998)". A new name was chosen to avoid suffixing saneroite so as to preserve *in toto* this "well-established name" and also to meet with the preferences of the collectors' community.

Braccoite also has a structural similarity with scheuchzerite, $NaMn_9^{2+}[Si_9V^{5+}O_{28}(OH)](OH)_3$ (Brugger *et al*., 2006; Palenzona *et al*., 2006; Roth, 2007): while saneroite/braccoite have a silicate single chain with five tetrahedra in the repeating unit – with an additional tetrahedron branching sideways (Fig. 5) – scheuchzerite has a chain that consists of the branched saneroite chain with additional attached silicate tetrahedra, forming "loops" (Brugger *et al*., 2006). These "loops" are also present in a new Na-Mn borosilicate, steedite $NaMn_2^{2+}[Si_3BO_9(OH)](OH)$ (IMA2013-052), of which the crystal structure resembles closely those of the serandite–pectolite pyroxenoids and is also broadly similar to the crystal structure of scheuchzerite (Haring and McDonald, 2014).

Braccoite is the first As member of the saneroite family and a comparison of the

https://doi.org/10.1180/minmag.2015.079.1.14 Published online by Cambridge University Press

TABLE 9. Comparison of minerals related to braccoite. References are given in brackets.

Reference	Braccoite (1)	Saneroite (2, 3)	Scheuchzerite (4)	Steedeite (5)
Formula	$NaMn_5^{2+}[Si_5AsO_{17}(OH)](OH)$	$NaMn_5^{2+}[Si_5VO_{17}(OH)](OH)$	$NaMn_9^{2+}[Si_9O_{25}(OH)(VO_3)](OH)$	$NaMn_2[Si_3BO_9](OH)_2$
Crystal system	Triclinic	Triclinic	Triclinic	Triclinic
Space group	$P\bar{1}$	$P\bar{1}$	$P\bar{1}$	$P\bar{1}$
a (Å)	9.7354(4)	9.741(5)	9.831(5)	6.837(1)
b	9.9572(3)	9.974(7)	10.107(5)	7.575(2)
c	9.0657(3)	9.108(5)	13.855(7)	8.841(2)
α (°)	92.691(2)	92.70(4)	86.222(10)	99.91(3)
β	117.057(4)	117.11(4)	73.383(9)	102.19(3)
γ	105.323(3)	105.30(4)	71.987(9)	102.78(3)
V (Å^3)	740.37(4)	744.16	1254.2(10)	424.81(1)
Z	2	2	2	2
Axial ratios (a:b:c)	0.978:1:0.910	0.977:1:0.913	0.973:1:1.371	0.9026:1:1.1671
D_{meas} (g cm^{-3})	n.d.	3.47	3.50(2)	n.d.
D_{calc} (g cm^{-3})	3.56	3.51	3.47	3.104
Strongest lines in the powder pattern: d_{obs} (Å)(I)	3.774(30), 3.514(30), 3.042(60), 3.005(60), 2.973(80), 2.821(100), 2.696(90), 2.620(30), 2.676(50), 1.673(30)	3.06(s), 2.83(s), 2.70(s), 3.01(m), 2.98(m), 2.62(m), 2.20(m)	2.71(100), 3.09(80), 7.91(70),8.68(50), 2.92(40), 3.22(40), 3.94(30), 4.83(30)	8.454 (100), 7.234(39), 3.331(83), 3.081(38), 2.859(52), 2.823(80)
Optical character	biaxial (+)	biaxial (−)	biaxial (+)	biaxial
Colour	brown-red	bright orange	yellow-orange	pale pink to colourless
Pleochroism	X = brownish yellow, Y = dark yellow, Z = yellow	X = deep orange; Y = lemon-yellow; Z = yellow-orange	X = brown yellow; Y = pale yellow	Not observed
Hardness (Mohs)	n.d.	n.d.	2–3	n.d.
Streak	pale-yellow	white	yellow-orange	white
Lustre	vitreous to resinous	resinous to greasy	vitreous	vitreous
Habit and forms	subhedral	tabular-prismatic crystals	acicular and prismatic crystals	acicular crystals
Association	aegirine, hematite, tiragalloite, quartz, unidentified Mn oxides and Mn silicates	quartz, baryte, caryopilite, ganophyllite, medaite, palenzonaite, pyrobelonite, fianelite, parsettensite, rhodochrosite, kutnahorite, aegirine	saneroite, tiragalloite	aegirine, analcime, cat-apleiite, eudialyte, microcline nepheline, natrolite, pyrrhotite, sérandite, sodalite, thermonatrite

Refs: (1) this work; (2) Lucchetti *et al.* (1981); (3) Nagashima and Armbruster (2010*a*); (4) Brugger *et al.* (2006); (5) Haring and McDonald (2014).

TABLE 10. Comparison of chemical data between saneroite from Molinello mine (Italy) and Fianel (Switzerland) and braccoite from Valleta (this work).

	Saneroite (Molinello mine, Italy)[1]				Saneroite (Fianel, Switzerland)[1]		Braccoite (Valletta mine, Italy)[2]	
	Specimen 1		Specimen 2					
	Wt.%	SD	Wt.%	SD	Wt.%	SD	Wt.%	SD
SiO_2	39.99	1.06	39.06	0.65	41.03	0.98	39.73	0.59
Al_2O_3	0.02	0	0.01	0.02	0.01	0.02	0.04	0.04
MnO	42.2	1.38	40.33	1.06	41.53	1.12	39.00	0.41
Mn_2O_3	–	–	–	–	–	–	3.07	0.53
MgO	0.01	0.02	0.00	0.00	0.03	0.04	0.96	0.05
CaO	0.13	0.05	0.11	0.04	0.33	0.12	0.05	0.01
Na_2O	4.34	0.28	4.36	0.27	4.52	0.25	4.06	0.2
K_2O	0	0.01	0.01	0.01	0.01	0.01	–	–
CuO	0.1	0.14	0.2	0.24	0.14	0.2	0.02	0.01
NiO	0.03	0.04	0.03	0.03	0.02	0.03	–	–
V_2O_5	7.15	1.8	7.78	0.7	6.05	1.23	1.43	0.11
As_2O_5	1.22	1.27	1.92	1.65	1.31	1.85	6.87	0.61
SO_3	–	–	–	–	–	–	0.01	0.01
F	–	–	–	–	–	–	0.04	0
Total	95.19		93.81		94.98		95.28	

Refs: (1) Nagashima and Armbruster (2010*a*); (2) this work.

properties of the members is reported in Table 9 along with other related structures. A comparison of published analyses of saneroite-group minerals is reported in Table 10. In the Strunz System (Strunz and Nickel, 2001) braccoite fits into subdivision 9.D.K, inosilicates with 5-periodic single chains. Its equivalent synthetic compound is not known.

Acknowledgements

The authors are indebted to Bruno Lombardo, who passed away some days after the identification of this new species, for his assessment support in fieldwork at the Valletta. Mariko Nagashima, Gerald Giester, Peter Leverett and Associate Editor Stuart Mills are thanked for their constructive comments on the manuscript. FC and EB thank MIUR and AMI for the co-funding of a research contract for EB for the year 2013. Raul Carampin (CNR-IGG, Padova, Italy) is thanked for his support with the WDS analysis.

References

Albee, A. and Chodos, A.A. (1970) Semiquantitative electron microprobe determination of Fe^{2+}/Fe^{3+} and Mn^{2+}/Mn^{3+} in oxides and silicates and its application to petrologic problems. *American Mineralogist*, **55**, 491–501.

Albrecht, J. (1990) An As-rich manganiferous mineral assemblage from the Ködnitz Valley (Eastern Alps, Austria): geology, mineralogy, genetic considerations, and implications for metamorphic Mn deposits. *Neues Jahrbuch für Mineralogie, Monatshefte*, 363–375.

Antofilli, M., Borgo, E. and Palenzona, A. (1983) *I nostri minerali. Geologia e mineralogia in Liguria*. SAGEP Editrice, Genova, 296 pp.

Barresi, A.A., Kolitsch, U., Ciriotti, M.E., Ambrino, P., Bracco, R. and Bonacina, E. (2005) La miniera di manganese di Varenche (Aosta, Italia nord-occidentale): ardennite, arseniopleite, manganberzeliite, pirofanite, sarkinite, thortveitite, nuovo As-Sc-analogo della metavariscite e altre specie. *Micro*, **3**, 81–122.

Basso, R. and Della Giusta, A. (1980) The crystal structure of a new manganese silicate. *Neues Jahrbuch für Mineralogie, Abhandlungen*, **138**, 333–342.

Borgo, E. and Palenzona, A. (1988) *I nostri minerali. Geologia e mineralogia in Liguria. Aggiornamento*. SAGEP Editrice, Genova, 48 pp.

Bracco, R. and Balestra, C. (2014) La miniera di Monte Nero, Rocchetta Vara, La Spezia, Liguria: minerali classici e novità. *Micro*, **12**, 2–28.

Bracco, R., Callegari, A., Boiocchi, M., Balestra, C.,

https://doi.org/10.1180/minmag.2015.079.1.14 Published online by Cambridge University Press

Armellino, G. and Ciriotti, M.E. (2006) Costa Balzi Rossi (Magliolo, Val Maremola, Savona, Liguria): una nuova località per minerali di Terre Rare e scandio. *Micro*, **4**, 161–178.

Bracco, R., Balestra, C., Castellaro, F., Mills, S.J., Ma, C., Callegari, A.M., Boiocchi, M., Bersani, D., Cadoni, M. and Ciriotti, M.E. (2012) Nuovi minerali di Terre Rare da Costa Balzi Rossi, Magliolo (SV), Liguria. *Micro*, **10**, 66–77.

Brown, I.D. (1981) The bond-valence method: an empirical approach to chemical structure and bonding. Pp. 1–30 in: *Structure and Bonding in Crystals II* (M. O'Keeffe and A. Navrotsky, editors). Academic Press, New York.

Brugger, J., Krivovichev, S., Meisser, N., Ansermet, S. and Armbruster, T. (2006) Scheuchzerite, $Na(Mn,Mg)_9[VSi_9O_{28}(OH)](OH)_3$, a new single-chain silicate. *American Mineralogist*, **91**, 937–943.

Cámara, F., Ciriotti, M.E., Bittarello, E., Nestola, F., Massimi, F., Radica, F., Costa, E., Benna, P. and Piccoli, G.C. (2014) As-bearing new mineral species from Valletta mine, Maira Valley, Piedmont, Italy: I. Grandaite, $Sr_2Al(AsO_4)_2(OH)$, description and crystal structure. *Mineralogical Magazine*, **78**, 757–774.

Chen, Y.L., Huang, C.H. and Hu, W.P. (2005) Theoretical study of the small clusters of LiH, NaH, BeH_2, and MgH_2. *The Journal of Physical Chemistry* A, **109**, 9627–9636.

Downs, R.T. (2006) The RRUFF Project: an integrated study of the chemistry, crystallography, Raman and infrared spectroscopy of minerals. *Program and Abstracts of the 19th General Meeting of the International Mineralogical Association in Kobe, Japan*, O03-13.

Franks, F. (editor) (1973) *Water: A Comprehensive Treatise*, **Vol. 2**. Plenum, New York, 684 pp.

Gramaccioli, C.M., Griffin, W.L. and Mottana, A. (1980) Tiragalloite, $Mn_4[AsSi_3O_{12}(OH)]$, a new mineral and the first example of arsenatotrisilicate. *American Mineralogist*, **65**, 947–952.

Hammer, V.M.F., Libowitzky, E. and Rossman, G.R. (1998) Single crystal IR spectroscopy of very strong hydrogen bonds in pectolite, $NaCa_2[Si_3O_8(OH)]$, and serandite, $NaMn_2[Si_3O_8(OH)]$. *American Mineralogist*, **83**, 569–576.

Haring, M.M.M. and McDonald, A.M. (2014) Steedeite, $NaMn_2[Si_3BO_9](OH)_2$: characterization, crystal-structure determination, and origin. *The Canadian Mineralogist*, **52**, 47–60.

Hatert, F., Mills, S.J., Pasero, M. and Williams, P.A. (2013) CNMNC guidelines for the use of suffixes and prefixes in mineral nomenclature, and for the preservation of historical names. *European Journal of Mineralogy*, **25**, 113–115.

Hawthorne, F.C., Abdu, Y.A., Ball, N.A and Pinch, W.W. (2013) Carlfrancisite: Mn_3^{2+} (Mn^{2+},Mg,Fe^{3+}, $Al)_{42}(As^{3+}O_3)_2(As^{5+}O_4)_4[(Si,As^{5+})O_4]_6[(As^{5+},Si)O_4]_2(OH)_{42}$, a new arseno-silicate mineral from the Kombat mine, Otavi Valley, Namibia. *American Mineralogist*, **98**, 1693–1696.

Horiba Jobin Yvon (2004, 2005) *LabSpec software for Raman spectroscopic data analysis, acquisition and manipulation. Version 5.64.15*. HORIBA Jobin Yvon SAS, Villeneuve d'Ascq, France.

Jacobsen, S.D., Smyth, J.R., Swope, R.J. and Sheldon, R.I. (2000) Two proton positions in the very strong hydrogen bond of serandite, $NaMn_2[Si_3O_8(OH)]$. *American Mineralogist*, **85**, 745–752.

Kimura, Y. and Akasaka, M. (1999) Estimation of Fe^{2+}/Fe^{3+} and Mn^{2+}/Mn^{3+} ratios by electron probe micro analyzer. *Journal of the Mineralogical Society of Japan*, **28**, 159–166 [in Japanese with English abstract].

Larson, A.C. and Von Dreele, R.B. (1994) *General Structure Analysis System (GSAS)*. Los Alamos National Laboratory Report LAUR, 86–748. Los Alamos National Laboratory, New Mexico, USA.

Libowitzky, E. (1999) Correlation of OH stretching frequencies and O–H···O hydrogen bond lengths in minerals. *Monatshefte für Chemie*, **130**, 1047–1059.

Lucchetti, G., Penco, A.M. and Rinaldi, R. (1981) Saneroite, a new natural hydrated Mn-silicate. *Neues Jahrbuch für Mineralogie, Monatshefte*, 161–168.

Mandarino, J.A. (1979) The Gladstone-Dale relationship. Part III. Some general applications. *The Canadian Mineralogist*, **17**, 71–76.

Mandarino, J.A. (1981) The Gladstone-Dale relationship. Part IV. The compatibility concept and its application. *The Canadian Mineralogist*, **19**, 441–450.

Marchesini, M. and Pagano, R. (2001) The Val Graveglia Manganese District, Liguria, Italy. *Mineralogical Record*, **32**, 349–379.

Mills, S.J., Frost, R.L., Kloprogge, J.T. and Weier, M.L. (2005) Raman spectroscopy of the mineral rhodonite. *Spectrochimica Acta*, **62**, 171–175.

Momma, K. and Izumi, F. (2011) "VESTA 3" for three-dimensional visualization of crystal, volumetric and morphology data. *Journal of Applied Crystallography*, **44**, 1272–1276.

Myneni, S.C.B., Traina, S.J., Waychunas, G.A. and Logan, T.J. (1998*a*) Experimental and theoretical vibrational spectroscopic evaluation of arsenate coordination in aqueous solutions and solids. *Geochimica et Cosmochimica Acta*, **62**, 3285–3300.

Myneni, S.C.B., Traina, S.J., Waychunas, G.A. and Logan, T.J. (1998*b*) Vibrational spectroscopy of functional group chemistry and arsenate coordination in ettringite. *Geochimica et Cosmochimica Acta*, **62**, 3499–3514.

Nagashima, M. and Armbruster, T. (2010*a*) Saneroite: chemical and structural variations of manganese

https://doi.org/10.1180/minmag.2015.079.1.14 Published online by Cambridge University Press

pyroxenoids with hydrogen bonding in the silicate chain. *European Journal of Mineralogy*, **22**, 393–402.

Nagashima, M. and Armbruster, T. (2010*b*) Ardennite, tiragalloite and medaite: structural control of $(As^{5+},V^{5+},Si^{4+})O_4$ tetrahedra in silicates. *Mineralogical Magazine*, **74**, 55–71.

Nakamoto, K. (1986) *Infrared and Raman Spectra of Inorganic and Coordination Compounds*. Wiley, New York, 419 pp.

Nickel, E.H. and Grice, J.D. (1998) The IMA Commission on New Minerals and Mineral Names: procedures and guidelines on mineral nomenclature, 1998. *The Canadian Mineralogist*, **36**, 913–926.

Palenzona, A. (1991) *I nostri minerali. Geologia e mineralogia in Liguria. Aggiornamento* 1990, p. 48. Amici Mineralogisti Fiorentini, Associazione Piemontese Mineralogia Paleontologia & Mostra Torinese Minerali, Centro Mineralogico Varesino, Gruppo Mineralogico "A. Negro" Coop Liguria (GE), Gruppo Mineralogico Lombardo, Gruppo Mineralogico Paleontologico "3M", SAGEP, Genoa, Italy [p. 48].

Palenzona, A. (1996) I nostri minerali. Geologia e mineralogia in Liguria, Aggiornamento 1995. *Rivista Mineralogica Italiana*, **2**, 149–172.

Palenzona, A., Martinelli, A., Bracco, R. and Balestra, C. (2006) IMA 2004-044 (scheuchzerite) alla miniera di Gambatesa. *Prie*, **2**, 11–12.

Pouchou, J.L. and Pichoir, F. (1984) A new model for quantitative analysis: Part I. Application to the analysis of homogeneous samples. *La Recherche Aerospatiale*, **3**, 13–38.

Pouchou, J.L. and Pichoir, F. (1985) 'PAP' φ(ρZ) procedure for improved quantitative microanalysis. Pp. 104–106 in: *Microbeam Analysis*. (J.T. Armstrong, Editor). San Francisco Press, San Francisco, USA.

Robinson, K., Gibbs, G.V. and Ribbe, P.H. (1971) Quadratic elongation: a quantitative measure of distortion in coordination polyhedra. *Science*, **172**, 567–570.

Roth, P. (2007) Scheuchzerite. Pp.130–131 in: *Minerals First Discovered in Switzerland and Minerals Named after Swiss Individuals*. Kristallografik Verlag, Achberg, Germany.

Shannon, R.D. (1976) Revised effective ionic radii and systematic studies of interatomie distances in halides and chaleogenides. *Acta Crystalographica*, **32**, 751–767.

Sheldrick, G.M. (2008) A short history of SHELX. *Acta Crystallographica*, **A64**, 112–122.

Strunz, H. and Nickel, E.H. (2001) *Strunz Mineralogical Tables. Chemical Structural Mineral Classification System*, 9th Edition. Schweizerbart, Stuttgart, 870 pp.

Wilson, A.J.C. (editor) (1992) *International Tables for Crystallography. Volume C: Mathematical, Physical and Chemical Tables*. Kluwer Academic Publishers, Dordrecht, The Netherlands.

Yvon, K., Jeitschko, W. and Parthé, E. (1977) LAZY PULVERIX, a computer program, for calculating X-ray and neutron diffraction powder patterns. *Journal of Applied Crystallography*, **10**, 73–74.

https://doi.org/10.1180/minmag.2015.079.1.14 Published online by Cambridge University Press